Nanoindentation of Biodegradable Cellulose Diacetate-*graft*-Poly(L-lactide) Copolymers: Effect of Molecular Composition and Thermal Aging on Mechanical Properties

SEUNG-HWAN LEE,[1] YOSHIKUNI TERAMOTO,[2] SIQUN WANG,[1] GEORGE M. PHARR,[3,4] TIMOTHY G. RIALS[1]

[1]Forest Product Center, Forestry, Wildlife and Fisheries, The University of Tennessee, Knoxville, Tennessee

[2]Biomass Technology Research Center, National Institute of Advanced Industrial Science and Technology, Hiroshima, Japan

[3]Department of Materials Science and Engineering, The University of Tennessee, Knoxville, Tennessee

[4]Metals and Ceramic Division, Oak Ridge National Laboratory, Oak Ridge, Tennessee

Received 20 June 2006; revised 19 November 2006; accepted 20 November 2006
DOI: 10.1002/polb.21074
Published online in Wiley InterScience (www.interscience.wiley.com).

ABSTRACT: Nanoindentation of cellulose diacetate-*graft*-poly(lactide)s (CDA-*g*-PLLAs) synthesized by ring opening graft copolymerization of L-lactide in bulk onto the residual hydroxyl positions on CDA were conducted to investigate the effect of the molecular composition and thermal aging on mechanical properties and creep behavior. Continuous stiffness measurement (CSM) technique was used to obtained hardness and elastic modulus. These material properties were expressed as a mean value from 100 to 300 nm depths and an unloading value at final indentation depth. The hardness and elastic modulus in all CDA-*g*-PLLAs were higher than those in pure CDA, indicating that the introduction of PLLA increases the hardness and elastic modulus. With an increase of crystallinity by thermal aging, the hardness and elastic modulus were increased in both CDA-*g*-PLLA and PLLA. The creep test performed by CSM showed that the creep strain of CDA was decreased by the grafting of PLLA. Thermal aging decreased the creep strain of CDA-*g*-PLLA and PLLA. With an increase of holding time, hardness was decreased, whereas elastic modulus was kept almost constant. © 2007 Wiley Periodicals, Inc. J Polym Sci Part B: Polym Phys 45: 1114–1121, 2007

Keywords: cellulose; continuous stiffness measurement; graft-copolymerization; graft copolymers; hardness; mechanical properties; nanoindentation; nanotechnology; poly(lactide)

INTRODUCTION

With the recent importance attached to "green" concepts, copolymerization and polymer blending of cellulose and its derivatives with synthetic biodegradable polymers, for example, aliphatic polyesters and copoly(ester-carbonate)s, have been actively investigated to produce novel multi-components polymers for extending their applications to bio-based high functional biodegradable thermoplastics.[1–11] In particular, graft-copolymerization could be one of the most promising ways to increase the utility of cellulose by incorporating different polymer ingredients at a mo-

Correspondence to: S.-H. Lee (E-mail: lshyhk@hotmail.com)

Journal of Polymer Science: Part B: Polymer Physics, Vol. 45, 1114–1121 (2007)

lecular structural level.[12,13] This leads to the desired control of general material properties, including biodegradability.[14–16]

Teramoto and Nishio have recently summarized their work on cellulose acetate-based graft copolymers.[17–19] They described the preparation of cellulose diacetate-based graft copolymers with a wide range of compositions and the effect of molecular parameters on mechanical and thermal properties. For instance, in tensile measurements conducted at 80–100 °C for sheets of melt-quenched cellulose diaceate-grafted poly(L-lactide)s (CDA-*g*-PLLAs), it was observed that the elongation increased drastically with increase of degree of molar substitution (MS) of lactyl unit. Thermal transition properties also varied depending on MS of lactyl unit, as represented by a drastic T_g depression with increasing MS ($0 < MS \leq 8$) and a subsequent crystallization of the PLLA side chains ($MS \geq 14$). Physical aging experiments showed that for aged copolymers with lower MSs of 4.7 and 22, the overall relaxation time and the distribution of relaxation times were, respectively, rather longer and much narrower compared with the corresponding data for plain PLLA. It was also found in crystallization experiments that the growth rate of spherulites in crystallized copolymers of MS 22–77 were much lower than that in PLLA, and the texture developed usually contained banded extinction rings, unlike the homopolymer PLLA.

The purpose of this study was to investigate the effect of the molecular composition and thermal aging of CDA-*g*-PLLAs on mechanical and creep behavior by nanoindentation with the continuous stiffness measurement technique. In fact, the CDA and PLLA are not a miscible polymer pair but are strongly incorporated mutually in nanoscopic order in CDA-*g*-PLLA copolymer, even though a material composed of an immiscible polymer pair on the nano-scale is generally difficult to be obtain. Furthermore, the brittle behavior of CDA-*g*-PLLA copolymers at room temperature makes their mechanical behavior difficult to fully characterized by means of conventional bulk mechanical tests. Therefore, tensile properties were collected at selected temperatures between 80 and 100 °C that spans the T_gs of CDA and PLLA homopolymer, as mentioned above.

Nanoindentation is a nearly nondestructive and sensitive method to provide valuable information about the morphology and mechanical properties of polymeric materials on the nano or submicron scale.[20–23] Especially, nanoindentation has become a very useful technique to search for quantitative structure-property correlations in multi-component polymeric materials.[24–26] In these materials, the mechanical properties of materials in fine spatial resolution depend on molecular orientation, degree of crystallinity, crystallite textures, and other morphologies formed.[24] For instance, the hardness in a poly(ethylene terephthalate) (PET)/poly(ethylene naphthalate) (PEN) blend is affected by thermal aging and PEN composition due to the crystallization development of PEN in the blend.[27]

EXPERIMENTAL

Materials

CDA was supplied by Daicel Chemical Industries. The degree of substitution was 2.15, and its degree of polymerization was about 160. The synthesis and characterization of the CDA-*g*-PLLAs have been described in a previous paper.[13] CDA-*g*-PLLAs with different molar substitution (MS), degree of polymerization (DP) and degree of substitution (DS) of lactyl unit, PLLA weight content (wPLLA), and PLLA weight content were coded as CDA-*g*-PLLA-1, -2, and -3. The values of molecular compositional parameters are listed in Table 1.

Thermal Aging

Different thermal treatments were conducted as the following. For quenching, the sample was heated at 220 °C on a Teflon sheet for 5 min in an oven under nitrogen atmosphere and was quickly cooled to 25 °C. For thermal aging, after heating to 200 °C and holding for 5 min, the sample was immediately transferred to another oven regulated at 123 °C and maintained there for 24 h. Table 2 shows thermal aging conditions, glass transition temperatures, and the relative crystallinity of the graft copolymer and PLLA employed in this work.

Preparation of Specimen for Nanoindentation

The quenched and thermally aged samples were cut into a small blocks and glued to an acrylic block for microtoming. The specimens (2-mm thick sheet) were cut in a direction parallel to the sheet surface using a glass knife. A final cut was

Table 1. Sample Code and Composition of Cellulose Diacetate-Grafted PLLAs used in this Study

Sample	Sample Code	Lactyl Unit			W_{PLLA} (%)
		MS	DP	DS	
Cellulose Diacetate	CDA	–	–	–	0
Cellulose Diacetate-Grafted Poly(L-lactide)	CDA-*g*-PLLA-1	3.8	5.7	0.670	51.6
	CDA-*g*-PLLA-2	6.9	9.7	0.714	66.0
	CDA-*g*-PLLA-3	57.9	80.5	0.719	94.2
Homopoly(L-lactide)	PLLA	–	–	–	100

MS, degree of molar substitution of lactyl unit; DP, average degree of polymerization of the lactyl side chains; DS, degree of lactyl substitution; W_{PLLA}, PLLA weight content.

made with a diamond knife to obtain a smooth surface. The root mean square (rms) surface roughness, obtained from the topography by AFM XE-100 (PSIA Inc.), was in the range of 10–20 nm for all specimens. Finally, the specimens were conditioned for at least 24 h at 21 °C and 60% relative humidity in the same room that housed the nanoindenter.

Nanoindentation

A Nano Indenter II (Nano Instruments), incorporating continuous stiffness measurement, was used for nanoindentation. Measurements involving a progressive series of loading and partial unloading cycles were conducted to a final indentation depth (300 nm), generating a series of hardness and modulus values as a function of the indentation depth. Ten experiments were conducted at 21 °C and 60% relative humidity at different locations on the samples. Nanoindentation was performed in six steps: approaching to surface, loading to peak load, holding the indenter at peak load, unloading to 90% of the peak load in 50 s, holding the indenter for 50 s, and finally, unloading completely.

The hardness (H) and the elastic modulus (E) can be calculated from the load-displacement data. Figure 1 shows the experimental schema for nanoindentation. Nanoindentation hardness is defined as follows:

$$H = \frac{P_{max}}{A}, \tag{1}$$

where P_{max} is the load measured at a maximum depth of penetration (h) in an indentation cycle and A is the projected contact area. As the indenter penetrates into the sample, both elastic and plastic deformation occurs and only the elastic portion of the displacement is recovered during unloading. The elastic modulus can be inferred from either the initial unloading contact stiffness (S), that is, the slope (dP/dh) of the initial portion of the unlading curve, or the stiffness measured by the continuous stiffness technique. A relation among contact stiffness, contact area, and elastic modulus can be derived as follows:

Table 2. Thermal Aging Conditions and Thermal Properties

Sample Code	Thermal Aging		T_g (°C)	Crystallinity, X_c	Stability Parameter, φ
	Temperature (°C)	Time (h)			
CDA-*g*-PLLA-3 (Q)	–	–	63.3	–	–
CDA-*g*-PLLA-3 (A)	123	24	66.9	0.329	0.44
PLLA (Q)	–	–	64.3	–	–
PLLA (A)	123	24	64.6	0.705	0.19

Q and A represent "quenched" and "thermally aged," respectively.

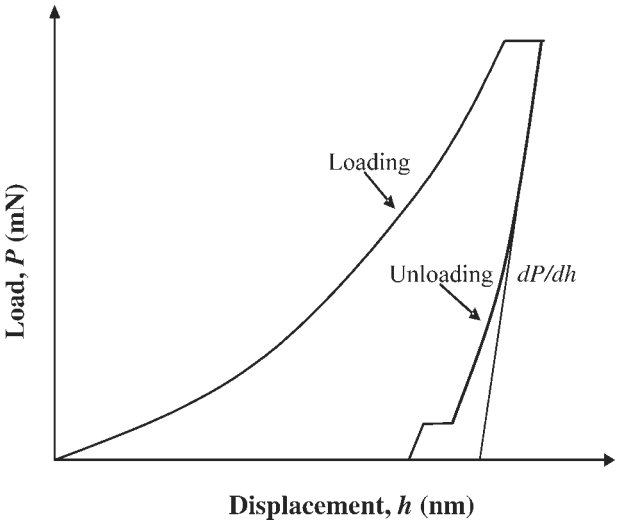

Figure 1. Experimental schema for nanoindentation.

$$S = 2\beta \sqrt{\frac{A}{\pi}} E_r, \tag{2}$$

where β is a constant that depends on the geometry of the indenter ($\beta = 1.034$ for a Berkovich indenter) and E_r is reduced elastic modulus, which accounts for the fact that elastic deformation occurs in both the sample and the indenter. The sample elastic modulus (E_s) can then be calculated as follows:[28]

$$E_s = (1 - \nu_s^2)\left\{\frac{1}{E_r} - \frac{1 - \nu_i^2}{E_i}\right\}, \tag{3}$$

where ν_s and ν_i (0.07) are the Poisson's ratios of the specimen and indenter, respectively, while E_i is the modulus of the indenter (1141 GPa). Poisson ratios of all samples used in this study were assumed to be 0.3.

Creep Experiment

The schema for nanoindentation creep experiment is shown in Figure 2. The indents were instantaneously made to achieve the final load. The final load was kept constant during a holding segment for 200 s. During holding segment, the series of indentation depth, hardness, and elastic modulus were monitored as a function of holding time.

RESULTS AND DISCUSSION

Effect of Molecular Composition on Hardness and Elastic Modulus

As mentioned in Introduction, the CDA-*g*-PLLA is so brittle at room temperature that its mechanical behavior is difficult to be fully characterized by means of common bulk mechanical tests at the temperature below T_g. Nanoindentation is capable to measure the mechanical properties in small area in a constrained manner, so the brittleness is not a critical factor in nanoindentation. Nanoindentation with continuous stiffness measurement used in this study provides an accurate and continuous record of indentation load and penetration depth during the indentation process. From the dependency of hardness and elastic modulus on indentation depth as shown in

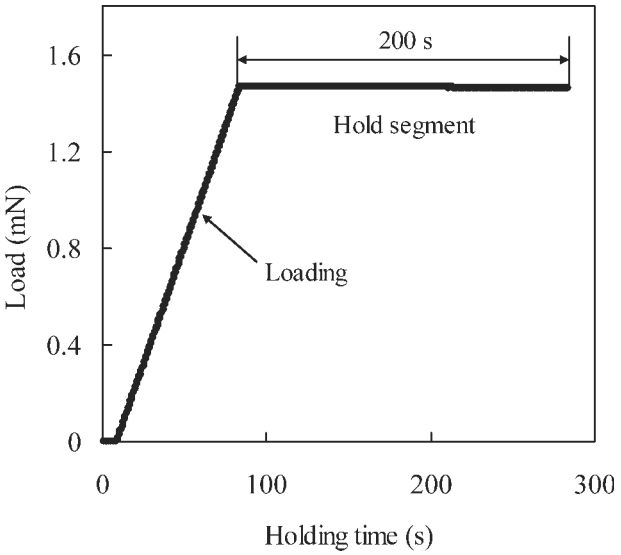

Figure 2. The schema for nanoindentation creep experiment.

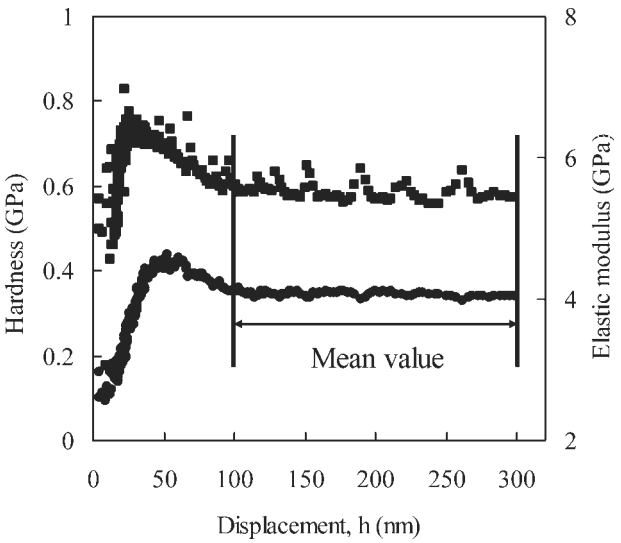

Figure 3. The dependency of hardness (●) and elastic modulus (■) on indentation depth. Sample code: CDA-*g*-PLLA-3(Quenched).

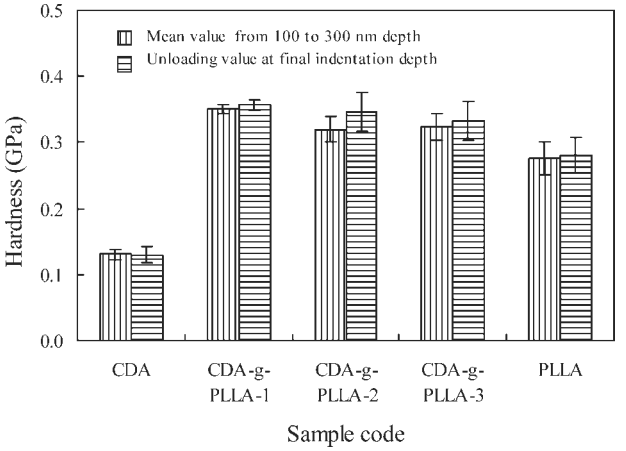

Figure 4. Hardness of CA, CDA-*g*-PLLAs with different MS and pure PLLA. All samples were quenched.

Figure 3, two different expressions for hardness and elastic modulus are possible. A mean value from 100 to 300 nm indentation depth and the unloading value at final indentation depth were obtained for hardness and elastic modulus.

Figures 4 and 5 show the values obtained for hardness and elastic modulus of CDA, CDA-*g*-PLLA with different MS and pure PLLA. The unloading value at the final indentation depth can be lower than the mean value, because of the creep effect during nanoindentation. In this study, however, there was no significant difference between two values, indicating that creep effect of these materials during nanoindentation is not critical. A statistical *t*-test revealed no significance at a confidence level of 0.95. All values for hardness and elastic modulus were higher in CDA-grafted PLLAs than in CDA and pure PLLA homopolymer. Such an increase of mechanical properties could be explained by the molecular structure of graft copolymer. PLLA itself has a relatively higher hardness and elastic modulus and its properties were further improved by incorporation with CDA, because CDA can play a role as a crosslinker and/or a structural sustainer of side chain PLLA with low molecular weight in CDA-*g*-PLLA. Both hardness and elastic modulus were lower in the CDA-*g*-PLLA with a higher MS than with a lower MS. The reason why CDA-*g*-PLLA with a higher MS shows a lower value for both hardness and elastic modulus could be that the lower content of grafting point in the high-MS copolymer induces the less frequent crosslinks and effect of the CDA sustainer for PLLA side chain.

Effect of Thermal Aging on Hardness and Elastic Modulus

In a previous study, it was described that PLLA side chain of CDA-*g*-PLAs with more than 14 of MS ($W_{PLLA} \geq 79$ wt %) becomes crystallizable at temperature above their respective glass transition temperature (T_g).[18] Thus, the CDA-*g*-PLLA with the MS of 57.9 was chosen to investigate the effect of crystallization on hardness and elastic modulus and pure PLLA was also used. Figures 6 and 7 show the effect of thermal aging on the mean value for hardness and elastic modulus of CDA-*g*-PLLA and pure PLLA. Hardness and elastic modulus were increased by developing

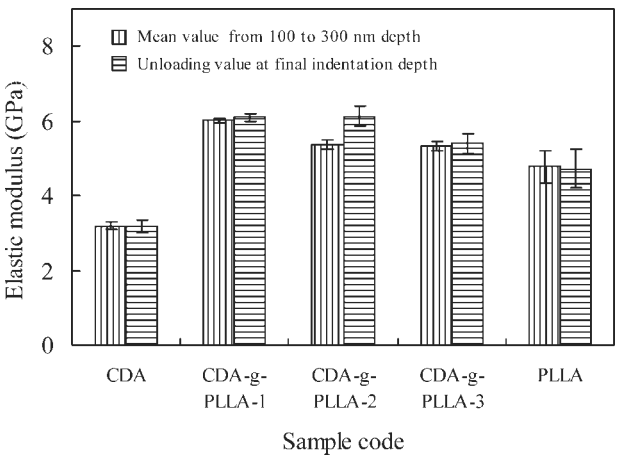

Figure 5. Elastic modulus of CA, CDA-*g*-PLLA with different MS and pure PLLA. All samples were quenched.

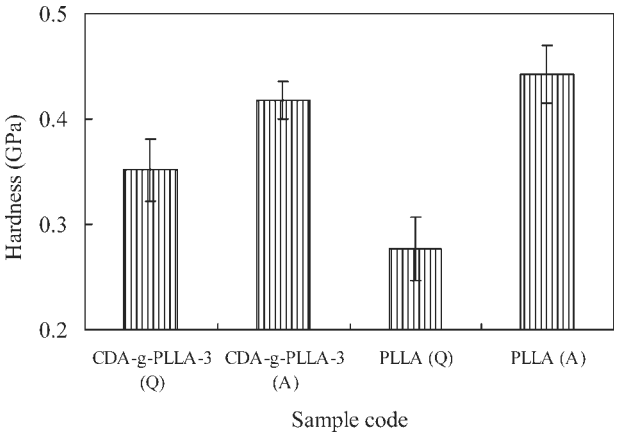

Figure 6. Effect of thermal aging on the mean value for hardness of CDA-*g*-PLLA and pure PLLA. Q and A represent "quenched" and "thermally aged," respectively.

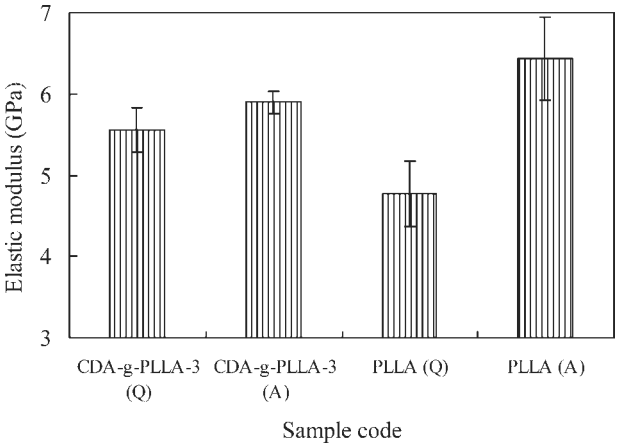

Figure 7. Effect of thermal aging on the mean value for elastic modulus of CDA-*g*-PLLA and pure PLLA. Q and A represent "quenched" and "thermally aged," respectively.

PLLA crystal in both samples, whereas the extent of the increase was higher in PLLA than in CDA-*g*-PLLA. This difference can be explained by the difference of the degree of relative crystallinity and crystal morphology. The relative crystallinity (X_c) of the PLLA fraction in CDA-*g*-PLLA copolymer was calculated by the following equation:

$$X_c = \frac{W_{PLLA}}{100} \cdot \frac{\Delta H}{93}, \quad (4)$$

where ΔH is the observed enthalpy of fusion and 93 (J/g of the polymer) is the enthalpy of melting of the PLLA crystal having the infinitely large crystal thickness, as reported by Fischer et al.[29]

The relative crystallinity of pure PLLA was higher than that of the CDA-*g*-PLLA (Table 2). Furthermore, a stability parameter of PLLA, which is related to morphological factors concerning the size and degree of perfection of the formed crystal, was higher than that of the CDA-*g*-PLLA. The PLLA side chains in CDA-*g*-PLLAs develop spherulites with different morphology than pure PLLA.[18] Banded extinction rings were observed during the spherulitic growth of CDA-*g*-PLLAs that were not present in the PLLA homopolymer. This phenomenon indicates that the molecular chains of PLLA were distorted in the spherulitic texture of the CDA-*g*-PLLAs. This is likely caused by the connection of PLLA molecular chain end onto the CDA backbone. The distortion of molecular chain alignment also may cause the decrease in relative crystallinity. The CDA fraction was incorporated into the interlamellar regions within the spherulites, without showing the segregation of the noncrystallizable CDA component in both the intraspherulitic region and the spherulitic contact region. This molecular chain distortion and the CDA incorporation into the interstitial regions of the spherulite may decrease the hardness and elastic modulus by nanoindentation.

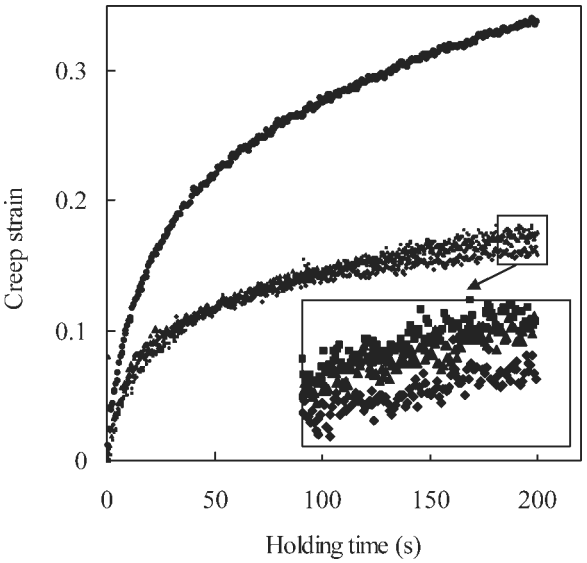

Figure 8. Effect of holding time on creep strain. Sample code: ● CDA, ■ CDA-*g*-PLLA-1, ▲ CDA-*g*-PLLA-2, ◆ CDA-*g*-PLLA-3, load 500 μN, loading rate 20 μN/s. All samples were quenched.

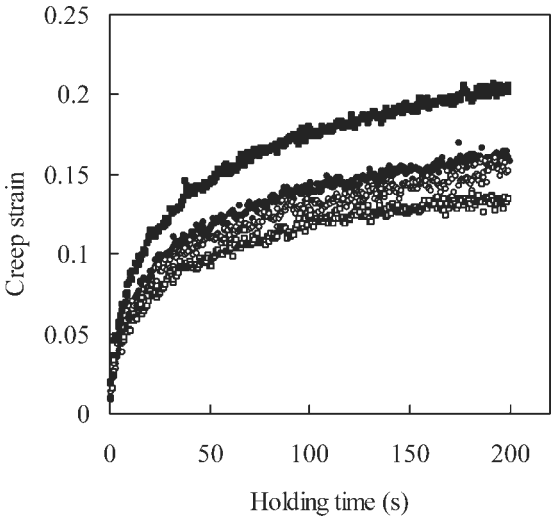

Figure 9. Effect of holding time on creep strain. Sample code: ● CDA-*g*-PLLA-3 (Q), ○ CDA-*g*-PLLA-3 (A), ■ PLLA (Q), □ PLLA (A), load 500 μN, loading rate 20 μN/s. Q and A represent "quenched" and "thermally aged," respectively.

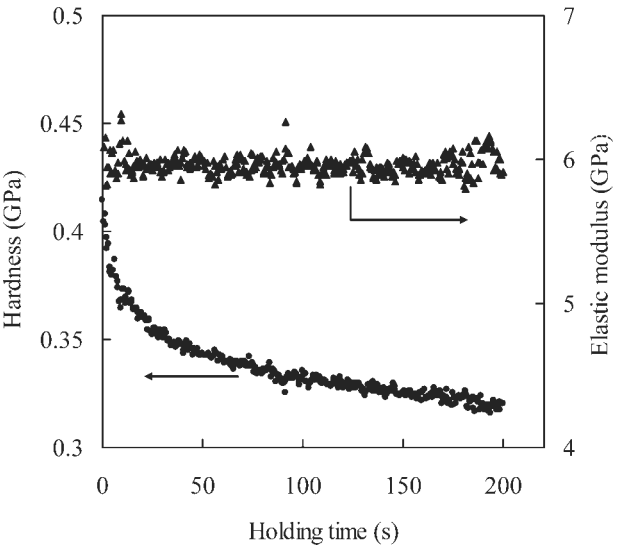

Figure 10. Effect of holding time on hardness and elastic modulus of CDA-*g*-PLLA. Sample code: CDA-*g*-PLLA-3 (A), load 500 μN, loading rate 20 μN/s.

Creep Behavior

Nanoindentation is a convenient method to estimate the creep behavior of materials, similar to conventional tensile or compression experiments. In depth sensing nanoindentation, creep behavior can be investigated by analyzing the change in nanoindentation displacement during holding time at a constant load. Figures 8 and 9 show the effect of holding time on creep strain, which is defined as the change in displacement during the holding time divided by the displacement at the start of the holding time. As shown in Figure 8, the creep strain was observed to be lower in CDA-*g*-PLLAs than in CDA, indicating that creep resistance is higher in CDA-*g*-PLLAs. This is because PLLA with a higher creep resistance is rich in copolymer. Among CDA-*g*-PLLAs, the CDA-*g*-PLLA with a higher MS of lactyl unit showed a high creep resistance. This can be the beneficial effect of the introduction of PLLA to reduce the creep deformation of CDA.

Figure 9 shows the effect of thermal aging on the creep strain. The creep deformation was decreased by thermal aging in both CDA-*g*-PLLA and pure PLLA. This higher creep resistance in thermally aged samples may be due to the crystallization of PLLA molecular chain. This result is consistent with the hardening phenomena by thermal aging as discussed above. A higher creep strain of the amorphous CDA-*g*-PLLA than PLLA homopolymer can occur by the incorporation of CDA with a large creep strain and a low molecular weight of the grafted PLLA side chain.

Figure 10 shows the relationship between the hardness and elastic modulus of CDA-*g*-PLLA3 (A) and the holding time at an applied load of 500 μN with a 20 μN/s loading rate. The hardness decreased as the holding time was increased. Elastic modulus was kept almost constant. This could be caused by crazing during the holding segment,and indicates that plastic deformation is more critical than elastic deformation for the holding time used in this study. For amorphous polymers, the free volume of a molecular chain is so small at temperature below T_g that the creep due to molecular motion should not be critical.[30] Under such a condition (amorphous and below T_g), creep behavior may be mainly attributed to crazing. This explanation for low hardness and almost the same elastic modulus during holding time seems reasonable for the given experimental conditions. All specimens displayed a similar phenomenon.

CONCLUSIONS

Mechanical properties of the CDA-*g*-PLLA copolymers are very difficult to be fully characterized by conventional bulk mechanical testing methods at room temperature because of their brittleness. However, the nanoindentation continuous stiffness measurement procedure used in this study was successful in investigating the mechanical properties and creep behavior of brittle materials at room temperature. The effects of the molecular composition and thermal aging on mechanical properties and creep behavior of CDA-*g*-PLLAs were investigated. The results showed that hardness and elastic modulus in all CDA-*g*-PLLAs were higher than those in pure CDA and were increased in both CDA-*g*-PLLA and PLLA with an increase of crystallinity by thermal aging. Creep experiment showed that the grafting of PLLA and thermal aging increased the creep resistance of CDA-*g*-PLLA and PLLA homopolymer. With an increase of holding time, hardness was decreased, whereas elastic modulus was kept almost constant.

The authors thank Y. Nishio of Kyoto University for providing the CDA-*graft*-PLLA samples along with the compositional data. The project was supported by the National Research Initiative of the USDA Cooper-

ative State Research, Education and Extension Service (grant number 2005-02,645) and the USDA Wood Utilization Research Grant. Instrumentation for the nanoindentation work was provided through the SHaRE Program at the Oak Ridge National Laboratory, which was sponsored by the Division of Materials Science and Engineering, US Department of Energy, under contract DE-AC05-000R22725 with UT-Battelle, LLC.

REFERENCES AND NOTES

1. Braganca, F. C.; Rosa, D. S. Polym Adv Technol 2003, 14, 669.
2. Buchanan, C. M.; Dorshel, D. D.; Gardner, R. M.; Komarek, R. J.; Matosky, J.; White, A. W.; Wood, M. D. J Environ Polym Degrad 1996, 4, 179.
3. Ceccorulli, G.; Pizzoli, M.; Scandola, M. Macromolecules 1993, 26, 6722.
4. El-Shafee, E.; Saad, G. R.; Fahmy, S. M. Eur Polym J 2001, 37, 2091.
5. Lee, S. H.; Yoshioka, M., Shiraishi, N. J Appl Polym Sci 2001, 81, 243.
6. Lee, S. H.; Wang, S. Polym Int 2006, 55, 292.
7. Miura, K.; Kimura, N.; Suzuki, H.; Miyashita, Y.; Nishio, Y. Carbohydr Polym 1999, 39, 139.
8. Miyashita, Y.; Suzuki, T.; Nishio, Y. Cellulose 2002, 9, 215.
9. Scandola, M.; Ceccorulli, G., Pizzoli, M. Macromolecules 1992, 25, 6441.
10. Teramoto, Y.; Ama, S.; Higeshiro, T.; Nishio, T. Macromol Chem Phys 2004, 205, 1904.
11. Wang, D. S.; Xuan, Y. N.; Huang, Y.; Shen, J. R. J Appl Polym Sci 2003, 89, 85.
12. Tetamoto, Y.; Yoshioka, M.; Shiraishi, N.; Nishio, Y. J Appl Polym Sci 2002, 84, 2621.
13. Teramoto, Y.; Nishio, Y. Polymer 2003, 44, 2701.
14. Hatakeyama, H.; Yoshida, T.; Hatakeyama, T. J Therm Anal Calorim 2000, 59, 157.
15. Lee, S. H.; Yoshioka, M.; Shiraishi, N. J Appl Polym Sci 2001, 77, 2908.
16. Videki, B.; Klebert, S.; Pukanszky, B. Eur Polym J 2005, 41, 1699.
17. Teramoto, Y.; Nishio, Y. Biomacromolecules 2004, 5, 407.
18. Teramoto, Y.; Nishio, Y. Biomacromolecules 2004, 5, 397.
19. Teramoto, Y.; Nishio, Y. Cellul Commun 2004, 11, 115.
20. Chua, S. M.; Henderson, P. J. J Mater Sci Lett 1991, 10, 1379.
21. Labour, T.; Ferry, L.; Gauthier, C.; Hajji, P.; Vigier, G. J Appl Polym Sci 1999, 74, 195.
22. Mina, M. F.; Ania, F.; Calleja, F. J. B.; Asano, T. J Appl Polym Sci 2004, 91, 205.
23. Seidler, S.; Koch, T. Macromol Symp 2004, 217, 329.
24. Zhu, S. H.; Chan, C. M.; Mai, Y. W. Polym Eng Sci 2004, 44, 609.
25. Flores, A.; Aurrekoetxea, J.; Gensler, R.; Kausch, H. H.; Calleja, F. J. B. Colloid Polym Sci 1998, 276, 786.
26. Zipper, P.; Janosi, A.; Geymayer, W.; Ingolic, E.; Fleischmann, E. Polym Eng Sci 1996, 36, 467.
27. Calleja, F. J. B.; Giri, L. J Mater Sci 1997, 32, 1117.
28. Oliver, W. C.; Pharr, G. M. J Mater Res 1992, 7, 1564.
29. Fischer, E. W.; Sterzel, H. J.; Wegner, G. Kolloid Z Z Polym 1973, 251, 980.
30. Nielsen, L. E. Mechanical Properties of Polymers and Composites; Marcel Dekker: New York, 1975.